Manuscript ID: MOLPHARM-AR-2020-000148R3

Metformin Prevents hyperglycaemia-associated, oxidative stress-induced vascular endothelial dysfunction: essential role for the orphan nuclear receptor, Nr4a1 (Nur77).

Vivek Krishna Pulakazhi Venu, Mahmoud Saifeddine, Koichiro Mihara, Muniba Faiza, Evgueni Gorobets, Andrew J. Flewelling, Darren Derksen , Simon A. Hirota, Isra Y. Marei, Dana Al-Majid, Majid Motahhary, Hong Ding, Chris R. Triggle and Morley D.Hollenberg

SUPPLEMENTAL FIGURE LEGENDS

Supplemental Figure 1: **Scheme showing the synthesis of biotinylated metformin.** The synthesis pathways, as outlined in Materials and Methods, show the production of biotinyl-metformin (Scheme 3) along with the synthesis of the two 'control' compounds, biotinylated 1-decylamine (the spacer arm for biotinylated metformin: Scheme 1) and metformin-decylamine, lacking the biotin tag (Scheme 2).

Supplemental Figure 2. Metformin protects against hyperglycaemia-induced increases in reactive oxygen species in murine microvascular endothelial cells. Mouse microvascular endothelial cell monolayers were cultured for 24 hours under conditions of either low (11 mM: panels A to C; G to I) or high (40 mM: Panels D to F; J to L) glucose. Cultures were supplemented or not with 50μM metformin (Panels G to L). Red fluorescence of the dihydroethidium indicator was taken as an index of ROS production shown by the representative micrographs. **Panels F** (without metformin) and **L** (with metformin) show the metformin-reduced ROS caused by high glucose (40 mM). **Panel M** shows the Image J analysis (histograms) of the fluorescence mean gray value of samples, relative to cells maintained in 11 mM glucose, was done to quantify the increase in ROS, and its reduction observed in the presence of metformin. * $P< 0.05$ for differences between mean gray values for 11 mM versus 40 mM glucose; and for 40 mM glucose without or with metformin. Histogram values represent the means +/- SEM (bars) for gray value ratios measured for 6 independent microscopic fields of the same area. Statistical significance was evaluated by ANOVA followed by a Bonferroni post-hoc test.

Supplemental Figure 3: Metformin protects mitochondrial respiration from hyperglycaemia in wild-type but not Nr4a1-null aorta tissues. Aorta rings from wild-type (A, B) and Nr4a1-null mice (C, D) were cultured in high-glucose (25 mM) for 24 hours in the presence (red bars) or absence (blue bars) of metformin (10μM). Cell monolayers were then evaluated with endothelial side facing up in the Seahorse assay chamber and assessed for their oxygen consumption rates (OCR) to evaluate the basal OCR along with spare respiratory capacity (panels A and C) as well as proton leak and ATP production (Panels B and D. **A and B:** Wild-type cells. **C and D:** Nr4a1-null cells. Histogram values represent the means, ±SD for n=5; $P<0.05$, comparing 25mMG/24h vs 25mMG/24 hours +10μM metformin for wild-type cells. There was no significant difference between the untreated and metformin-treated Nr4a1-null cells.

Supplemental figure 4: Metformin improves extracellular acidification rate (ECAR), an indicator of glycolysis in wild-type endothelial cells. Mouse aortic endothelial cells were incubated with 25mM glucose for 24 hours without (blue symbols) or with either 10 μM metformin (red symbols) or 500μM metformin (purple symbols). The data show ECAR measurements following the sequential addition of glucose, oligomycin and 2-deoxyglucose. Data points represent the mean ECAR values ±SEM (bars) for n=6 monolayers per condition. Error bars smaller than the symbols are not shown.

Supplemental figure 5: Lack of effect of metformin to upregulate Nr4a1 mRNA in intact hyperglycaemia-exposed aorta rings and lack of effect of actinomycin D to prevent metformin from improving hyperglycaemia-impaired vascular vasodilator function in vitro. Aorta rings were subjected to organ culture under hyperglycaemic conditions (25 mM glucose: HG) for 48 hours and then mounted in the wire myograph as for a bioassay, described in Methods. The organ bath Krebs buffer was then supplemented or not with either 100 µM (Panel A) or 10 µM metformin (Panel B) in the absence or presence of 1 µM actinomycin D (AD). **PANEL A.** After 3 hours in the organ bath at 37 °C, tissues were harvested and processed for qPCR measurements of the abundance of Nr4a1 mRNA relative to that of GAPDH, as outlined in methods. **PANEL B.** After 3 hours in the organ bath the vasodilator actions of 3 µM ACh were measured. Histogram values represent the means +/- SEM for measurements with three tissues for qPCR and for 4 tissues for the vasorelaxation responses expressed as a % of the tension generated by 2.5 µM phenylephrine (% PE contraction).

Supplemental figure 6: *In silico* predicted interactions of cytosporone B and celastrol with NR4A1. UPPER PANEL, CYTOSPORONE B: (A) Representation of NR4A1 (cartoon model) interacting with cytosporone B (stick model). (B) Active site residues interacting with cytosporone B (blue ball and stick model) along with bond lengths. (C) Surface representation of Nr4a1 pocket within which cytosporone B fits. **LOWER PANEL, CELASTROL:** (A) Representation of NR4A1 (cartoon model) interacting with celastrol (stick model). (B) Active site residues interacting with celastrol (blue ball and stick model) along with bond lengths. (C) Surface representation of Nr4a1 pocket within which celastrol lies.

Supplemental figure 7: *In silico* predicted interactions of THPN with NR4A1. A) Representation of Nr4a1 (cartoon model) interacting with THPN (stick model). **B)** Active site residues interacting with THPN (blue ball and stick model) along with bond lengths. **C)** Surface representation of NR4A1 pocket within which lies the THPN.

Supplemental figure 8: *In silico* predicted interactions of TMPA with NR4A1. A) Representation of Nr4a1 (crystallographic ribbon model) interacting with TMPA5f (stick model). **B)** Active site residues interacting with TMPA (blue ball and stick model) along with bond lengths. **C)** Surface representation of TMPA situated in the Nr4a1 ligand binding pocket.

Scheme 1. Synthesis of biotin-tagged-1-decylamine (1)

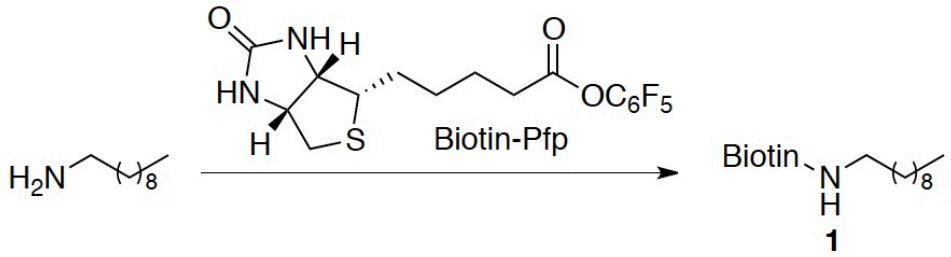

Scheme 2. Synthesis of metformin-decylamine (3)

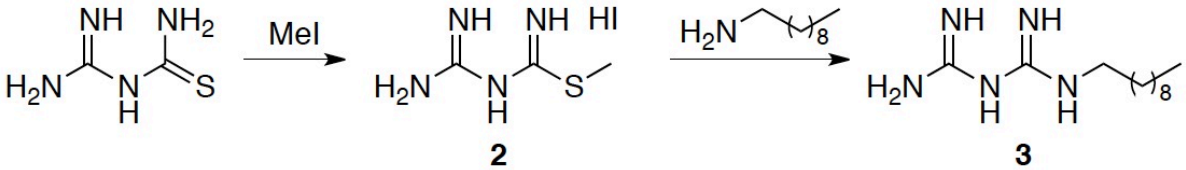

Scheme 3. Synthesis of biotin-tagged metformin (4)

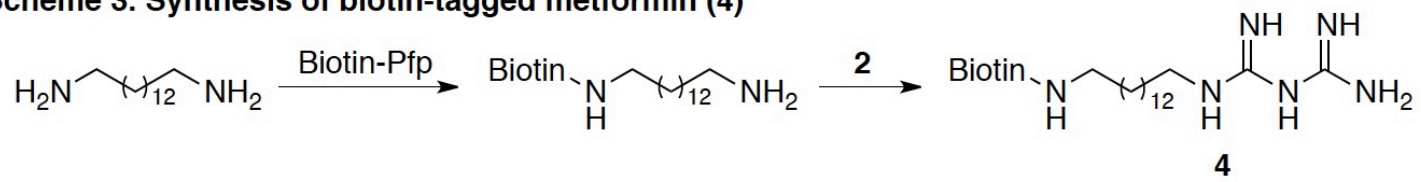

Supplemental Figure 1

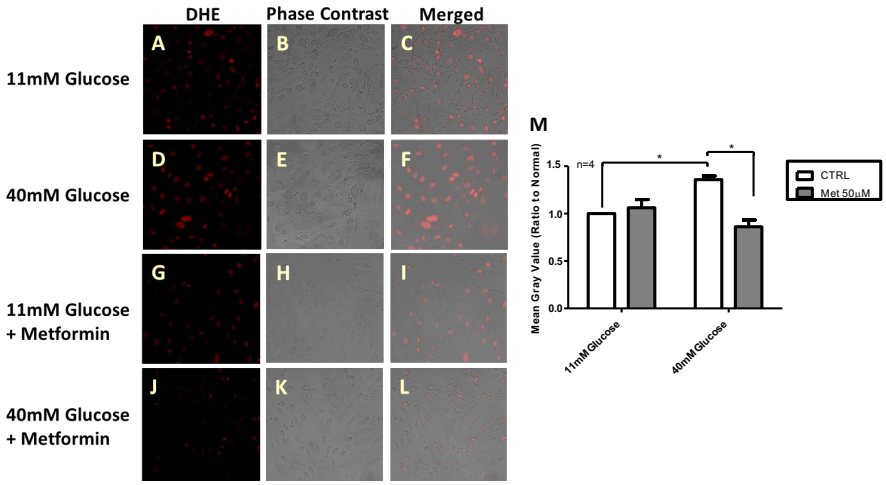

Supplemental Figure 2

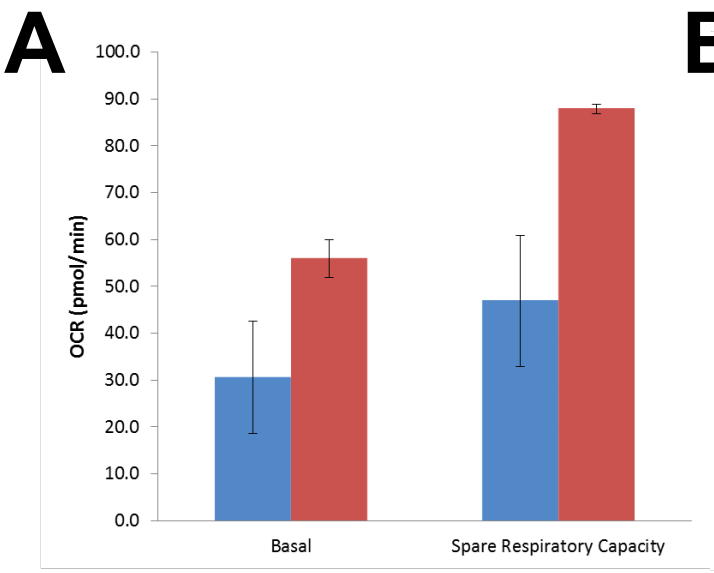

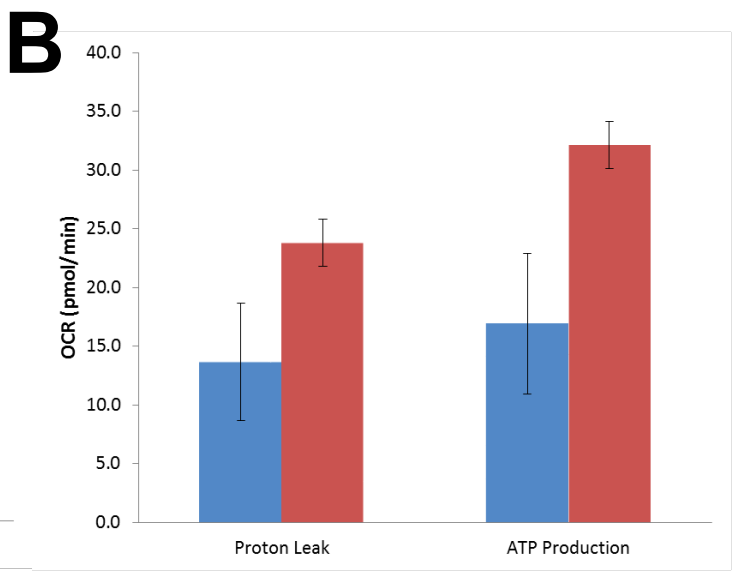

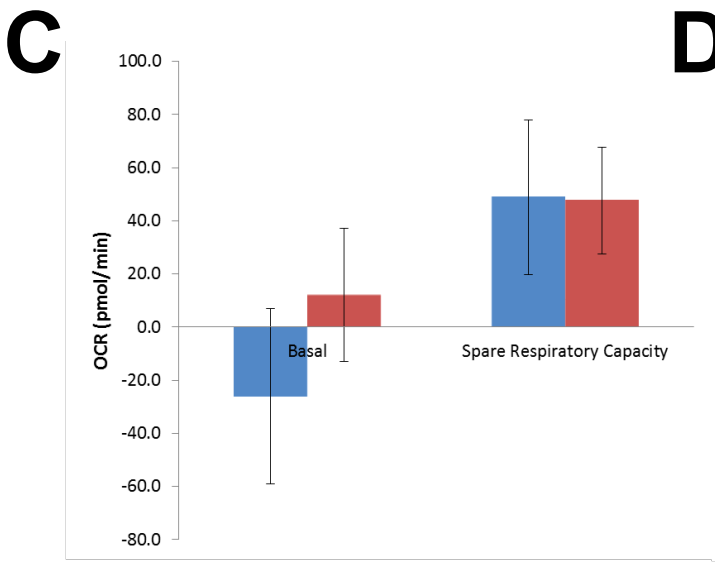

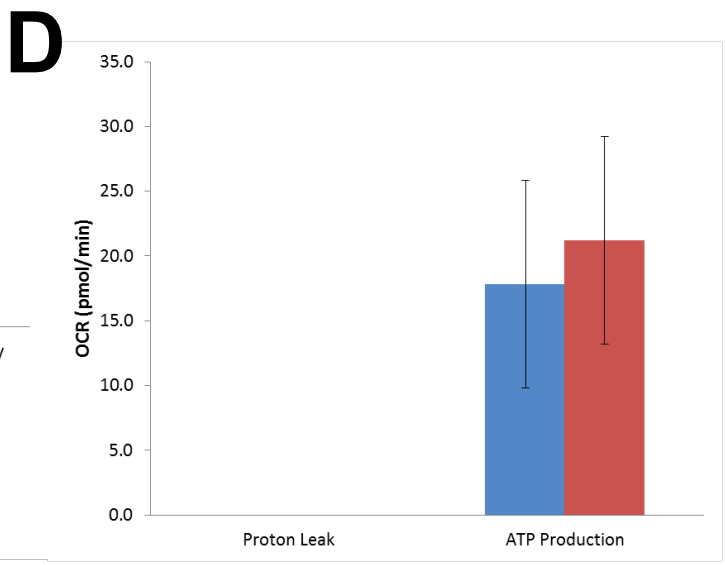

Supplemental Figure 3

A

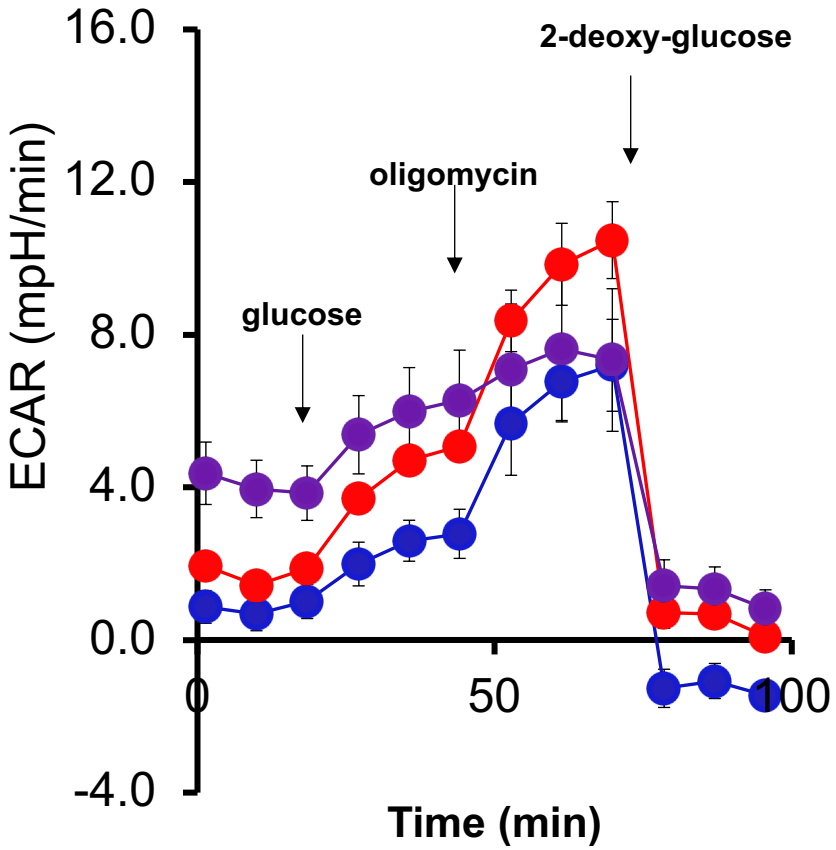

Supplemental Figure 4

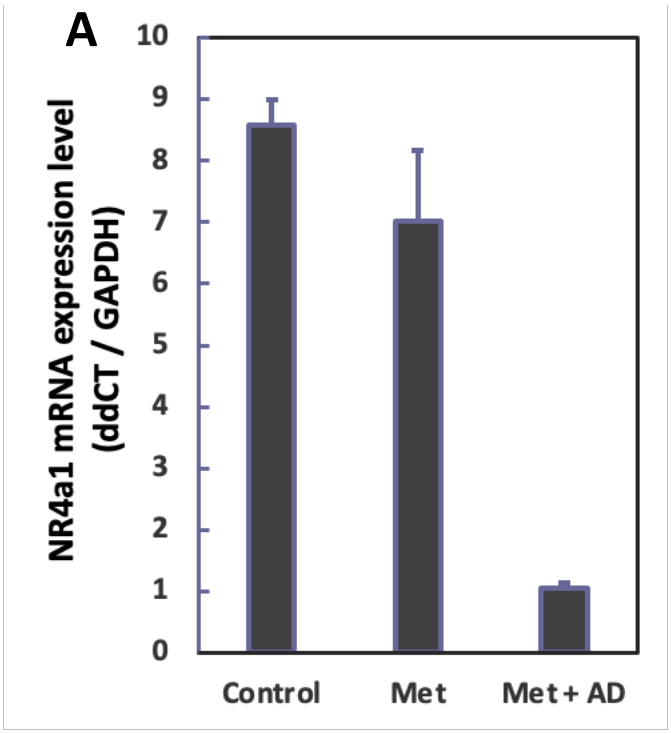

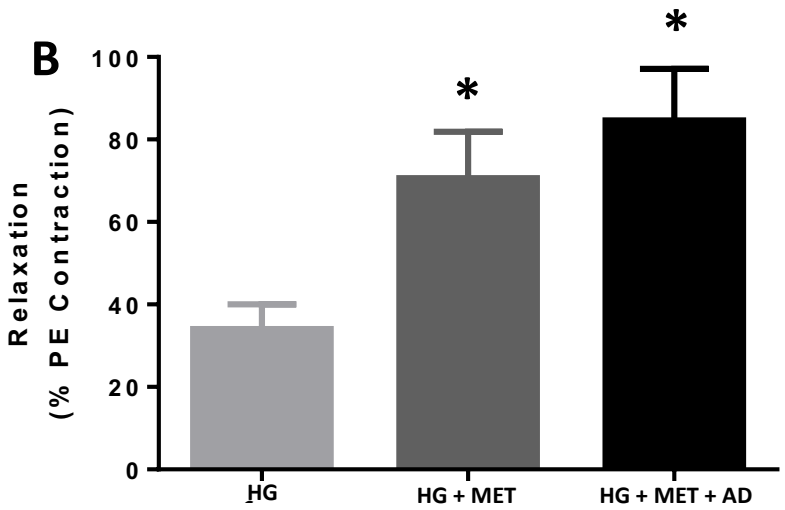

Supplemental Figure 5

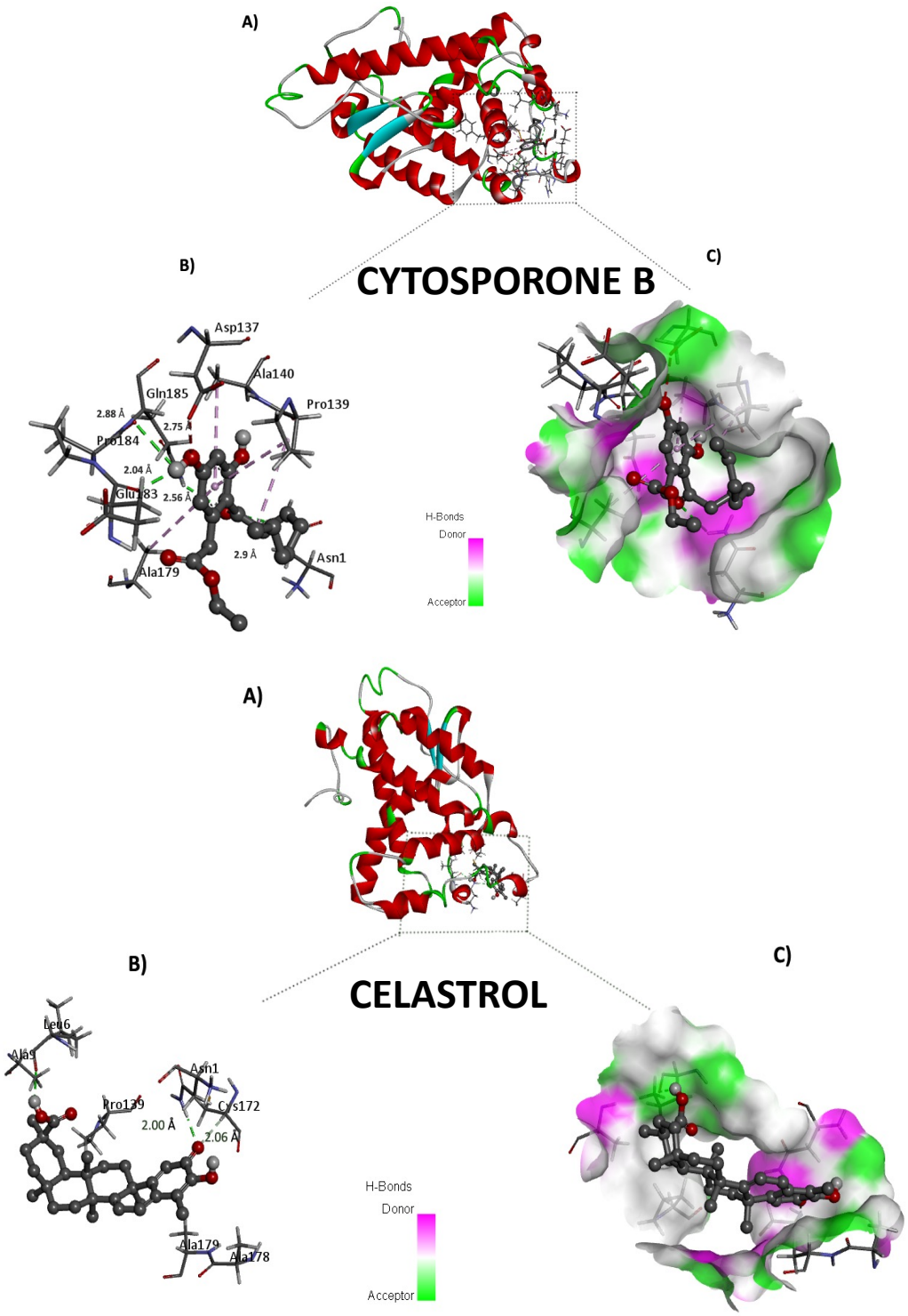

Supplemental Figure 6

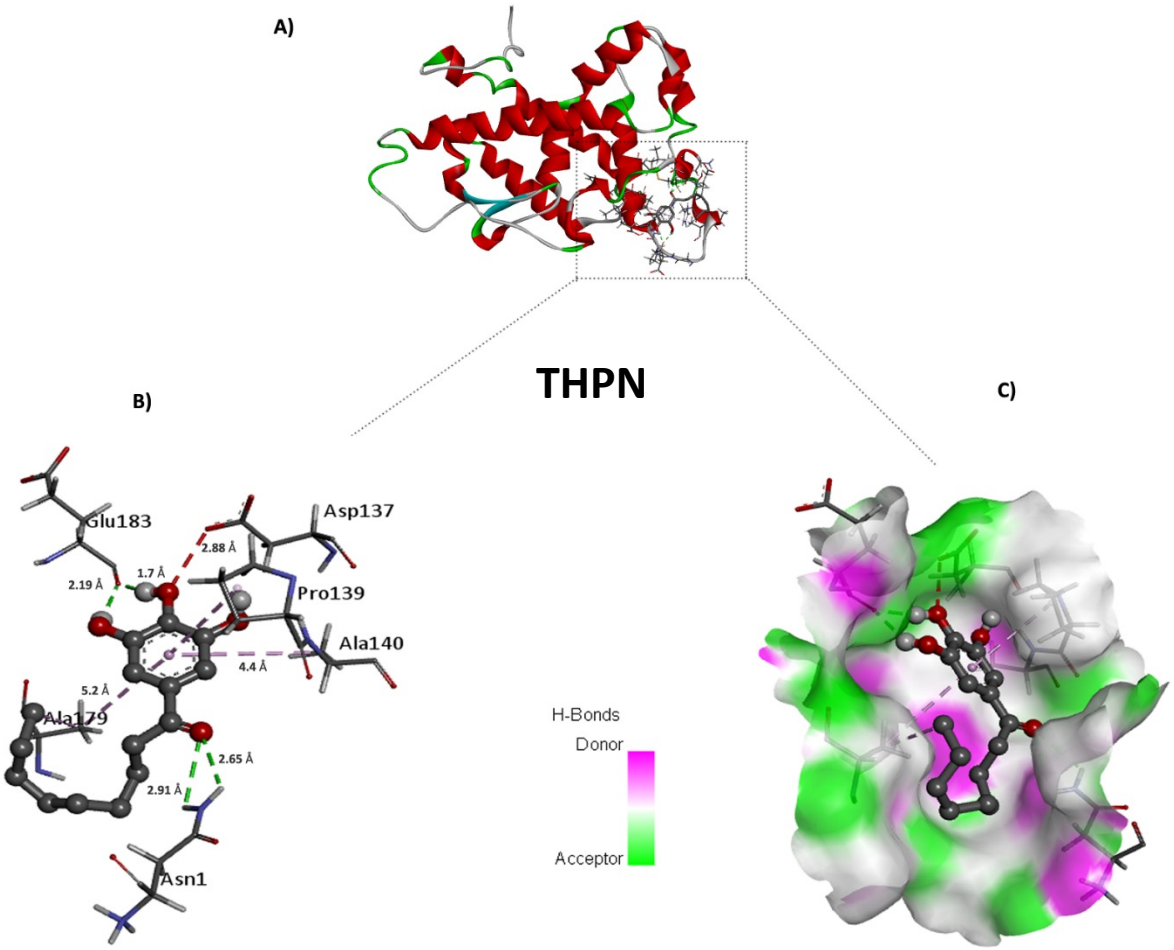

Supplemental Figure 7

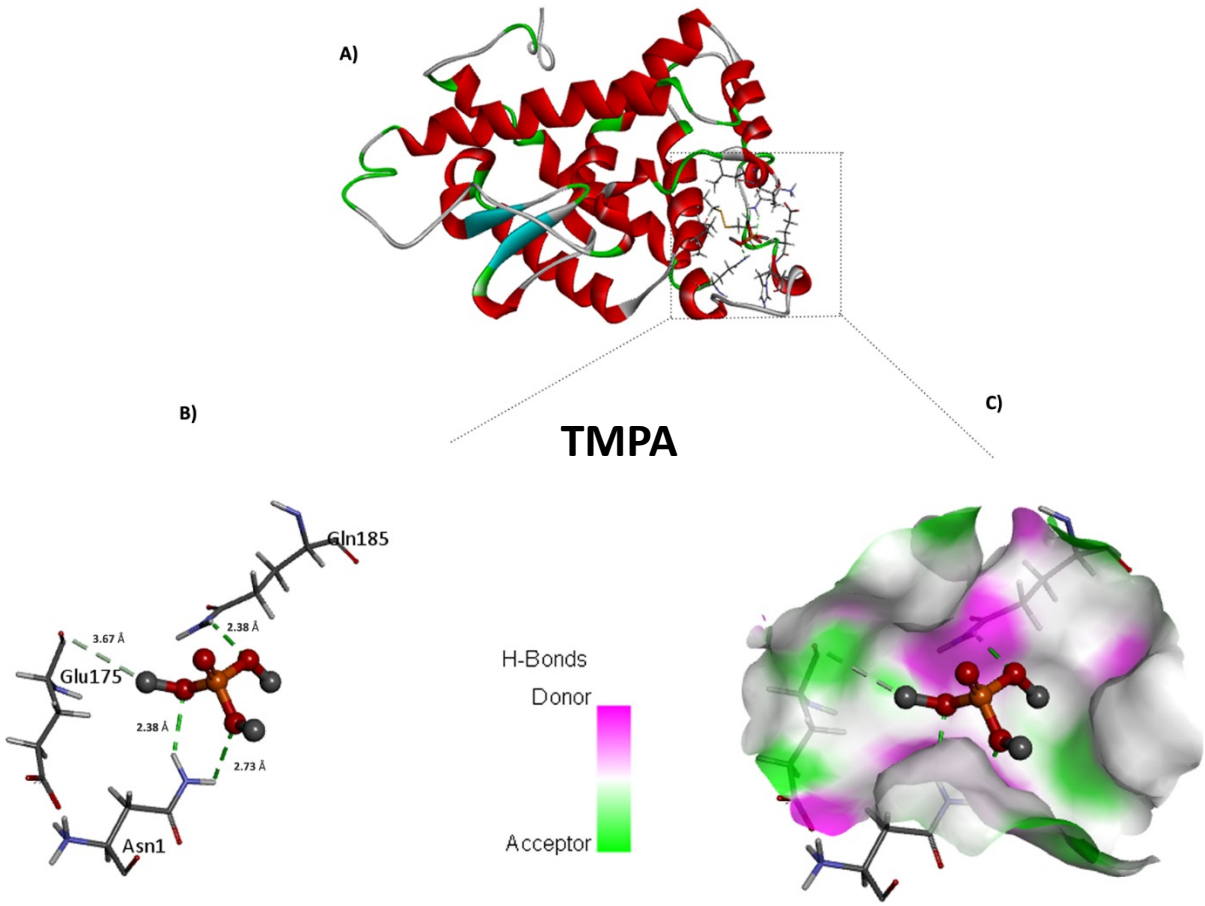

Supplemental Figure 8